

# PASSIVE FAULT TOLERANT CONTROL: A BOND GRAPH APPROACH

Nacusse, Matías A.<sup>(a,b)</sup> and Junco, Sergio J.<sup>(a)</sup>

<sup>(a)</sup>LAC, Laboratorio de Automatización y Control, Departamento de Control, Facultad de Ciencias Exactas, Ingeniería y Agrimensura, Universidad Nacional de Rosario, Ríobamba 245 Bis – S2000EKE Rosario – Argentina.

<sup>(b)</sup> CONICET – Consejo Nacional de Investigaciones Científicas y Técnicas.

<sup>(a,b)</sup>[nacusse@fceia.unr.edu.ar](mailto:nacusse@fceia.unr.edu.ar), <sup>(a)</sup>[sjunco@fceia.unr.edu.ar](mailto:sjunco@fceia.unr.edu.ar)

## ABSTRACT

The Passive Fault Tolerant Control (PFTC) approach defines a unique, robust control law able to achieve the control objectives even in the presence of a fault. This work addresses the PFTC problem in the Bond Graph (BG) domain. The control law is obtained using an energy and power shaping method in this domain. At its first step, the method proposes a so called Target Bond Graph (TBG) that expresses the desired closed-loop behaviour, i.e., the control system specifications, in terms of a desired closed-loop storage function and a power dissipation function. The control law is obtained in a subsequent step via BG-prototyping. In order to make it fault-tolerant, this control law is further robustified by using a residual signal obtained from a modified version of the diagnostic bond graph (mDBG) which is created from the TBG. This results in a closed-loop behavior under faults that is asymptotically equivalent to the faultless case.

Keywords: Passive Fault Tolerant Control, Bond Graph, Energy and Power Shaping, Diagnostic Bond Graph.

## 1. INTRODUCTION

Fault tolerant control (FTC) can be classified in two main categories, Passive Fault Tolerant Control (PFTC) and Active Fault Tolerant Control (AFTC). The passive approach defines a unique control law to achieve the control objectives even in the presence of a fault. Generally speaking, the passive approach ensures stability and confers robustness under faults to the control system, but there exists a trade-off between performance and robustness (Isermann 2006). The active approach modifies the control law according to the faults occurred, so that in this approach the faults must be detected and isolated and a decision must be made in order to reconfigure the control law. Both approaches are usually complemented in the praxis to improve the performance and stability of the fault tolerant system (Blanke, et al. 2006). Refer to (Zhang and Jiang 2008) for a bibliographical and historical review on FTC.

There are many methods for model based FDI defined in the BG domain. Most of these methods derive analytical redundant relations (ARR) from the BG

model (Ould Bouamama et al. 2003) and other use the BG model for direct numerical evaluation of ARRs (Samantaray et al. 2006), (Borutzky 2009).

This work addresses the problem of Passive Fault Tolerant Control (PFTC) in the BG domain. To obtain the fault tolerant control law, an energy and power shaping method in the BG domain is used (Junco 2004). This method first expresses the control system specifications in terms of desired closed-loop energy and power dissipation functions, capturing them in a so called Target Bond Graph (TBG) matching the desired closed-loop behaviour. The method proceeds further constructing the control inputs to the plant via Bond Graph prototyping in such a way that the coupling of the resulting controller-BG (a BG representing the control law) and the plant-BG is equivalent to the TBG.

The classic approach to solve problems of system parameter dispersion and to simultaneously reject disturbances is adding integral action to the controller (Khalil 1996). The BG solution to this problem presented in (Junco 2004) has been generalized in a Port-Controlled Hamiltonian Theory context in (Donaire and Junco 2009). This previous result is shown in this paper to solve a PFTC problem, but yielding a closed-loop response different than the originally defined in the TBG. In this paper, a new control law based on a modified Diagnostic Bond Graph (mDBG) is proposed. It makes the closed-loop system behave like the original TBG, at least asymptotically.

As presented in (Samantaray et al. 2006) the Diagnostic Bond Graphs (DBG) are originally used to generate residuals for fault detection and isolation (FDI) in Active Fault Tolerant Control (AFTC) problems. The standard version of the DBG uses the plant inputs and the plant measurements to generate a residual signal. This residual signal depends on the model parameters and the real plant parameters. Here, a modified version of the DBG is proposed: instead of feeding the plant nominal model with the measurements, the original TBG, i.e., the nominal control system, is fed with the actual reference signals and measured plant outputs. Thus, the residual signal obtained from the mDBG is a measure of the error between the desired and the actual dynamics of the control system. If the residual signal is

zero, then the control system behaves like the TBG and the control objectives are achieved. So, the control law aims at making the residual signal vanish in time.

The methodology proposed here is developed through a case study and validated numerically in simulation using the software 20sim (Controllab Products B.V).

The rest of the paper is organized as follows. Section 2 presents the system under study, its mathematical model and some background results necessary to introduce the contributions of the paper. Section 3 presents the methodology contributed by the paper illustrated through an example. Section 4 presents some simulation responses that prove the good dynamic response of the control system. Section 5 addresses some issues related to controller reconfiguration and, finally, in Section 6, conclusions and future work are addressed.

## 2. BACKGROUNDS

This section presents the system under study and some background on the energy and power shaping method in the BG domain.

### 2.1. System under study

The system under study, depicted in Figure 1a, consists of two tanks located one above the other, where the upper tank discharges into the lower tank.

The tanks are fed with one input flow which is splitted between them through a distribution valve whose parameter  $\gamma \in [0,1]$  determinates how the input flow is distributed to the tanks, if  $\gamma = 1$  then all the input flow is directed to the upper tank.

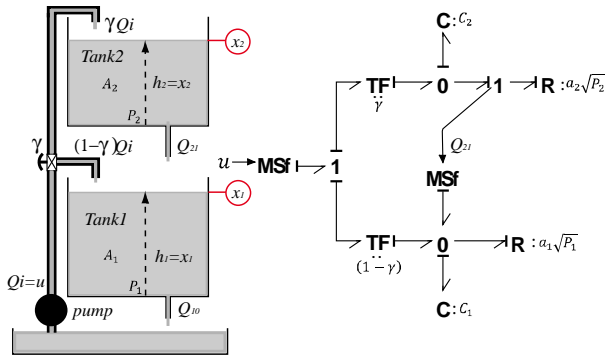


Figure 1. Physical system and its BG model. Measured plant outputs encircled in red.

The state equations can be read from the BG using the stored liquid volumes as state variables, as usual, or the liquid levels, as done here in (1):

$$\begin{aligned} \dot{x}_1 &= -\frac{a_1\sqrt{\rho g x_1}}{A_1} + \frac{a_2\sqrt{\rho g x_2}}{A_1} + \frac{(1-\gamma)}{A_1} u \\ \dot{x}_2 &= -\frac{a_2\sqrt{\rho g x_2}}{A_2} + \frac{\gamma}{A_2} u \end{aligned} \quad (1)$$

Where  $x_1$  and  $x_2$  represents the liquid level of tank1 and tank2 respectively;  $A_1$  and  $A_2$  are the cross section areas of the tanks, related to the tanks hydraulic

capacities by the relation  $C_i = \frac{A_i}{\rho g}$  (with  $i=1,2$ );  $\rho$  is the constant density of the liquid,  $g$  is the gravitational acceleration and  $a_1$  and  $a_2$  represents the cross section of outlet hole from the tanks.

Observing the BG model of Figure 1 it is easy to see that the system is structurally state controllable, because all states are input-reachable which means there exist a causal path between the source and every energy store in integral causality, and the energy storage elements can change causality when derivative causality is preferred (Sueur and Dauphing-Tanguy 1991) (this being a result valid for linear systems can be applied to a version of our BG linearized around an equilibrium point). Moreover, the tank level  $x_1$  can be achieved through two different causal paths. The shorter comes directly from the modulated source through the transformer (input-to-state relative degree 1). The other causal path comes from the modulated flow source over tank2 (input-to-state relative degree 2). So, the state variable  $x_1$  is input-reachable by two different paths; this structural redundancy can be used in case of faults in the distribution valve. Indeed, even for a severe fault like  $\gamma = 1$ , i.e., for a complete obstruction of the lower duct, which directly feeds tank1, the system is still structurally state controllable.

Let  $x_1$  and  $x_2$  be the measures of the system making it observable. In steady state condition the system imposes the following constraint:

$$\bar{x}_2 = \left(\frac{\gamma a_1}{a_2}\right)^2 \bar{x}_1 \quad (2)$$

This steady state constraint allows controlling one tank level forcing the other level to a desired value. This dependency can be used in case of sensor faults.

The faults considered in this work can be classified in three different groups:

- Faults in the constitutive relationships of the BG components, for example an obstruction / opening of the discharges orifices.
- Structural faults, for example an obstruction in the distribution valve ( $\gamma = 1$  or  $\gamma = 0$ ), Leakage in one or both tanks.
- Sensor faults.

### 2.2. Power and Energy shaping on bond graphs

The power and energy shaping control technique defines the control problem as a stabilization one, imposing the desired closed-loop energy and power dissipation, and obtaining the control law through matching equations relating the control open-loop energy function (a kind of control Lyapunov function, see Sontag 1998) and the desired closed-loop functions.

In the BG domain the desired stored energy and power dissipation are captured in the TBG. In order to obtain the control law, the controlled sources in the BG model of the plant are prototyped with the aim of obtaining a so called virtual BG that matches the TBG. For further details the reader must refer to (Junco 2004).

This method is exemplarily performed on the discussed two tank model with the following control objectives on tank1:

- Level tracking.
- Disturbance rejections.
- Robustness regarding parametric uncertainties.

The proposed TBG for the closed loop system is shown in Figure 2 with the desired stored energy and power dissipation expressed in terms of the tracking error state variable in (3) and (4). To simplify the notation in the equations the following constants have been introduced:  $k_1 = (\rho g)^2 C_1$ ,  $k_2 = \frac{(\rho g)^2}{R_H}$ , where  $R_H$  represents a hydraulic resistance and  $C_1$  a tank hydraulic capacity.

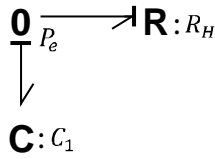


Figure 2. Proposed TBG

$$V(x) = \frac{1}{2} k_1 x_e^2 \quad (3)$$

$$\dot{V}(x) = -k_2 x_e^2 \quad (4)$$

In the equations above, the tracking error  $x_e = x_1 - x_1^{ref}$  is the state variable of the (incremental) TBG,  $x_1^{ref}$  is the tank1 reference level, and  $b = \frac{k_2}{\rho g}$ .

To enforce the desired closed-loop dynamics specified by the TGB, the virtual BG of Figure 3 is constructed. It shows how to proceed in order to obtain the control law. The left half of the figure is obtained prototyping the controlled power source  $MS_f$  in such a way that access is gained to the chosen output, the level  $x_1$ , and an overall equivalent behavior to the TBG is achieved (some cancellations can be seen following the causal paths, also note that there are some virtual elements with negative “gains”).

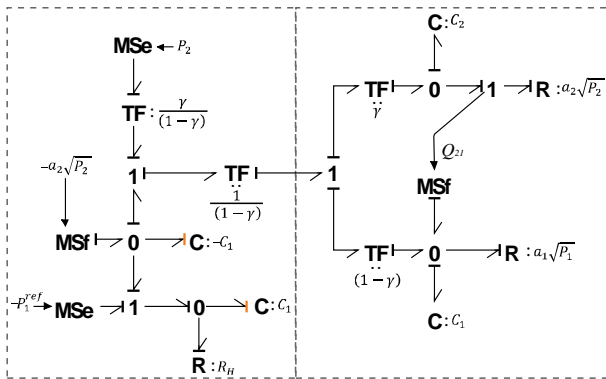


Figure 3. Virtual BG.

Using the standard causality reading procedure, the control law (5) is obtained directly from the virtual BG. This law can be thought of splitted into three components as in (6). The first and second term cancel the perturbation from tank2 and the nonlinearity of the outlet flow of tank1, respectively, and the third imposes the tracking error desired dynamics.

$$u = \left(\frac{1}{1-\gamma}\right) [-a_2 \sqrt{\rho g x_2} + a_1 \sqrt{\rho g x_1} - b(x_1 - x_1^{ref}) + A_1 \dot{x}_1^{ref}] \quad (5)$$

$$u = \left(\frac{1}{1-\gamma}\right) [u_1 + u_2 + u_3] \quad (6)$$

$$u_1 = -a_2 \sqrt{\rho g x_2}, \quad u_2 = a_1 \sqrt{\rho g x_1}, \\ u_3 = -b(x_1 - x_1^{ref}) + A_1 \dot{x}_1^{ref}$$

Assuming exact model knowledge and perfect measurements, this control law yields a closed-loop behavior equivalent to the TBG of Figure 2, i.e., the closed-loop dynamics satisfies (7). As no objectives are imposed on tank2 and its dynamics is hidden in closed-loop, its stability must be analyzed after the controller has been designed, property that can be easily verified in this case.

$$\dot{x}_e = -\frac{b}{A_1} x_e \quad (7)$$

*Perturbed closed-loop dynamics.* Because of parameter dispersion, faults, modeling errors, sensor limited precision, noise, etc., neither the model nor the measurements are exact. To deal with this it is convenient to think the control input as composed by two terms as in (8), where  $u_r$  is the “rated” part of  $u$ . This means the control input part that performs the power and energy shaping under ideal plant and measurement conditions. In the same expression,  $\delta_u$  is the unknown controller part due to modeling errors, parametric dispersion, faults, etc. The BG of Figure 4 reflects this situation.

$$u = u_r + \delta_u \quad (8)$$

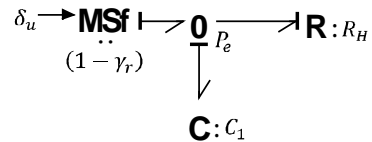


Figure 4. Perturbed TBG

Under this situation the closed-loop dynamics no longer satisfies (7) but (9), where  $\gamma_r$  is the rated value of the distribution valve parameter:

$$\dot{x}_e = -\frac{b}{A_1} x_e + \frac{(1-\gamma_r)}{A_1} \delta_u \quad (9)$$

It can again be verified that the hidden closed-loop dynamics of tank 2 is stable as it satisfies (10):

$$\dot{x}_2^{CL} = -\frac{a_2\sqrt{\rho g x_2}}{(1-\gamma_r)A_2} + \frac{a_1\gamma_r\sqrt{\rho g x_1}}{(1-\gamma_r)A_2} - \frac{b\gamma_r(x_1-x_1^{ref})}{(1-\gamma_r)A_2} + \frac{A_1\gamma_r\dot{x}_1^{ref}}{(1-\gamma_r)A_2} + \frac{\gamma}{A_2}\delta_u \quad (10)$$

It can be seen in (9) that the level error of tank 1 is driven by  $\delta_u$ . A remedy must be found if this induces inadmissible behavior in closed-loop. The next subsection shows how to do this in the BG domain using existing results. The solution is shown to be good even under the presence of some faults. In the next section a new result is presented which recovers a closed-loop performance closer to that of the original TBG.

### 2.3. Robustifying the control law adding integral action.

Looking at the perturbed TBG of Figure 4 a solution comes immediately to mind: inject a state-dependent flow into the 0-junction that (asymptotically) cancels the flow injected by the disturbance source. This is attained adding the I-element as shown in Figure 5, which is exactly adding integral action to the control law, a classic approach to solve problems of system parameter dispersion and to simultaneously reject disturbances (Khalil 1996). This kind of BG solution first presented in (Junco 2004) has been theoretically generalized in the context of the Port-Controlled Hamiltonian Systems Theory in (Donaire and Junco, 2009).

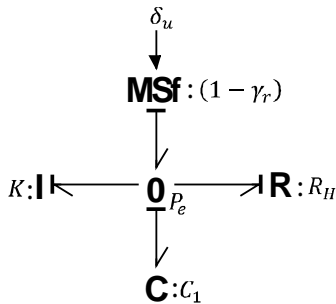


Figure 5. Perturbed TBG with integral action

The control law with integral action has to be calculated on the modified TBG given in Figure 6. Proceeding in the same way as when deriving equation (5) the control law  $u = \left(\frac{1}{1-\gamma}\right)[u_1 + u_2 + u_3 + u_4]$  is obtained, with  $u_4 = K \int (x_1 - x_1^{ref})$ .

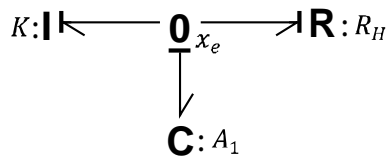


Figure 6. TBG with integral action

The tracking error  $x_e$  can be shown to satisfy (11), ie., a second order dynamics is obtained which differs

from the first order dynamics error defined by the TBG of Figure 2. Note however that this second order dynamics can be made to arbitrarily close approximate a first order dynamics with the correct choice of  $\frac{b}{A_1}$  (i.e.,  $R_H$ ) and  $K$ , at least theoretically, then this is mathematically possible but physically limited by the capacity of the actuators.

$$\ddot{x}_e + \frac{b}{A_1}\dot{x}_e + Kx_e = \frac{(1-\gamma_n)}{A_1}\delta_u \quad (11)$$

### 2.4. Diagnostic Bond Graph

The Diagnostic Bond Graph was first presented by (Samantaray et al. 2006) for numerical evaluation of analytical redundant relationships (ARR). The ARRs are calculated to perform FDI in an AFTC frame.

Basically, the DBG is obtained from a BG model of the plant injecting the plant measurements and inputs through modulated sources. The residual signal is obtained by measuring the power co-variables of the modulated sources, see Figure 7.

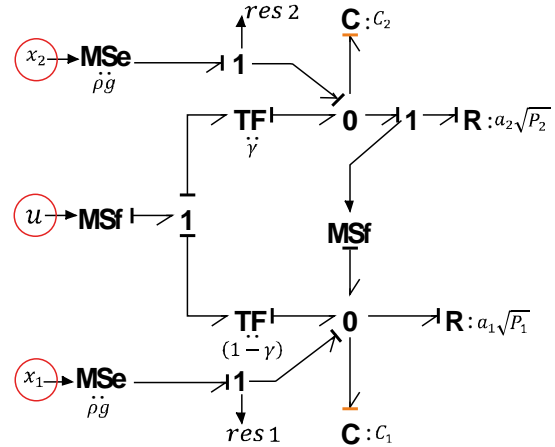


Figure 7. Diagnostic Bond Graph. Plant measurements to be fed into the DBG encircled in red.

Reading directly from the BG the residuals are:

$$\begin{aligned} res1 &= A_1\dot{x}_1 + a_1\sqrt{\rho g x_1} + a_2\sqrt{\rho g x_2} - (1-\gamma)u \\ res2 &= A_2\dot{x}_2 + a_2\sqrt{\rho g x_2} - \gamma u \end{aligned} \quad (12)$$

As can be noted in (12), the residuals depend on system parameters. If the model represents perfectly the controlled system, then the residual signals are zero. The derivative causality is an advantage in FDI, because no initial states are necessary to evaluate the residuals.

In the sequel only residual 1 is considered, as it is the only one related to the TBG associated to the control problem the paper deals with.

### 3. MAIN RESULT

In this section, the residual signal obtained from a modified version of the DBG is used to obtain a control law which is robust to faults.

### 3.1. Modified Diagnostic Bond Graph (mDBG).

The mDBG is defined injecting the tracking error level (as measured on the real control system) into the TBG through modulated sources, see Figure 8.

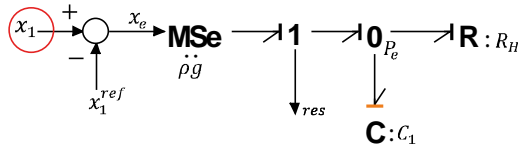


Figure 8. Proposed mDBG. Measurements to be fed into the mDBG encircled in red.

The mDBG yields the new error dynamics in (13), where  $res$  is the residual signal read from the mDBG, a measure of the difference between the actual and the ideally expected closed-loop dynamics. This signal is used to make the control law more reliable under faults.

$$\dot{x}_e = -\frac{b}{A_1}x_e + \frac{res}{A_1} \quad (13)$$

As it can be seen in (13), the error dynamics is driven by the residual signal, when  $res = 0$ ,  $x_e$  responds as previously defined in the TBG of Figure 2.

### 3.2. Obtaining the control law.

The control objective is reached when there exists a control law  $u = u(x_1, x_2, x_1^{ref}, res)$  such that  $res$  tends to zero with growing time.

The residual expression (14) obtained reading the mDBG clearly shows that choosing  $u$  as in (5) yields  $res = 0$  in absence of faults and modeling errors.

$$res = -a_1\sqrt{\rho gx_1} + a_2\sqrt{\rho gx_2} + b(x_1 - x_1^{ref}) - A_1\dot{x}_1^{ref} + (1 - \gamma)u \quad (14)$$

To compensate for faults and improve the control system robustness, the extra term  $u_4$  shown in (15) is added to the expression (5) for  $u$ .

$$u = \left(\frac{1}{1-\gamma}\right) [-a_2\sqrt{\rho gx_2} + a_1\sqrt{\rho gx_1} - b(x_1 - x_1^{ref}) + A_1\dot{x}_1^{ref} + u_4] \quad (15)$$

Choosing  $u_4 = -K \int res$  yields the residual dynamics (16):

$$res + Kres = (1 - \gamma_n) \delta_u \quad (16)$$

Thus, with constant  $\delta_u$ ,  $res$  goes asymptotically to zero with time constant  $1/K$ . As already anticipated, this forces  $x_e$  to approach asymptotically the desired error dynamics defined in the TBG of Figure 2.

Representing  $u_4$  in terms of  $(x_1 - x_1^{ref})$  yields (17), expression showing that, in this case, the residual signal defined in the mDBG has a PI structure. Note however that this does not necessarily generalize, since the resulting structure depends on the TBG.

$$u_4 = -KA_1(x_1 - x_1^{ref}) - Kb \int (x_1 - x_1^{ref}) \quad (17)$$

## 4. SIMULATIONS RESULTS

The parameters used in the simulations are:  $A_i = 28 \text{ cm}^2$ ,  $\rho = 2 \frac{gr}{\text{cm}^3}$ ,  $g = 981 \frac{\text{cm}}{\text{s}^2}$  and  $a_i = 0.71 \text{ cm}^2$  (Johansson 2000),  $b = 1$ ,  $K = 1$ ,  $\gamma = 0.5$ ,  $\gamma_r = 0.45$ . The control law given in (15), (17) is used.

The simulation scenario concerns abrupt faults in the system and the measurements are noise free.

The dynamic response of the control system with different faults occurring at time  $T = 75\text{s}$  is shown in Figures 9–13. As can be seen from these figures,  $x_1$  recovers its reference level  $x_1^{ref} = 30\text{cm}$  after the fault occurrence, and the residual signal, which is sensitive to the faults considered, tends to zero while  $x_2$  remains bounded.

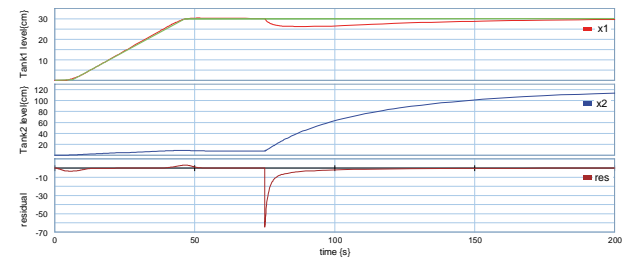


Figure 9. 75% obstruction in the outlet hole of tank2

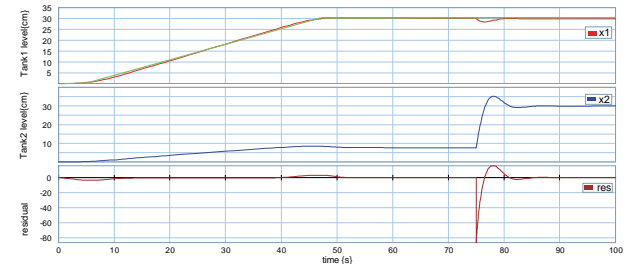


Figure 10. Fault in the distribution valve,  $\gamma = 1$

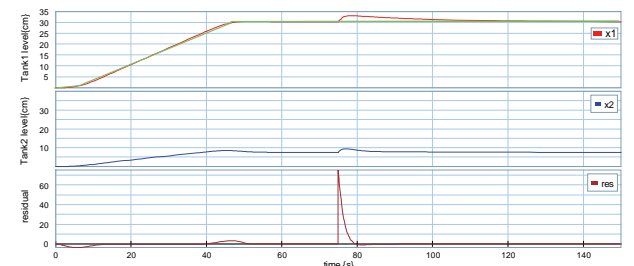


Figure 11. Fault in the level sensor of tank2, measured level equal to zero.

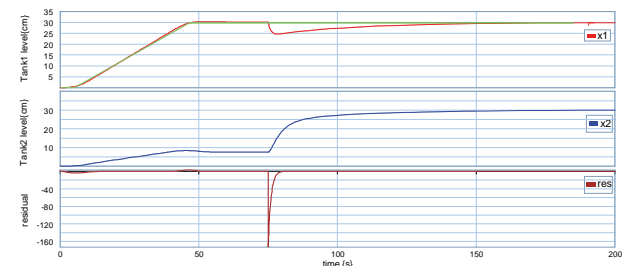


Figure 12. Leakage in tank1.

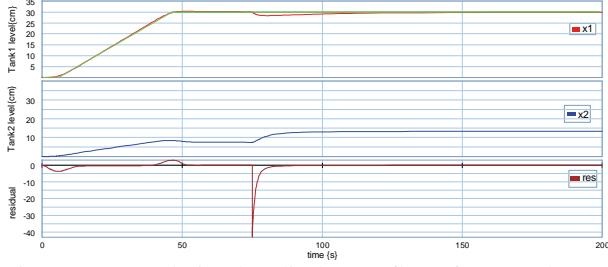


Figure 13. Fault in the discharge flow from tank2 to tank1, only 50% enters into tank1.

Figure 14 shows the dynamical response of the controlled system under multiple sequential faults. The simulation scenario is as follows, at time  $T = 75s$  a 75% obstruction in the outlet hole of tank2 happens, at time  $T = 250s$  the distribution valve fails ( $\gamma = 1$ ), at time  $T = 400s$  the level sensor of tank2 measures 50% of its actual value, at time  $T = 550s$  a leakage in tank1 appears with outlet hole cross section  $0.6 \text{ cm}^2$ , finally, at time  $T = 700s$  only the 50% of the outlet flow of tank2 enters into tank1.

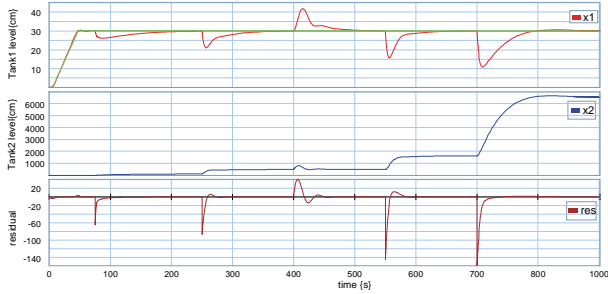


Figure 14. Multiple sequential faults.

As seen in the figures above, the control system is fault tolerant under different faults scenarios. However, this fault tolerance depends on the tank2 capacity, i.e., no overflow is modeled, in a real case tank2 could overflow. In such a case the controller should be reconfigured to manage the faults.

Figure 15 shows the behavior under a simultaneous fault occurrence at time  $T = 75s$  in the distribution valve and in tank2 outlet hole ( $\gamma = 1$  and 75% obstruction, respectively). Some measurement noise (normal distribution and amplitude  $n = 0.1 \text{ cm}$ ) has been considered. In this case the controller again rejects the faults forcing the tank1 level to follow its reference and the residual signal remains close to zero.

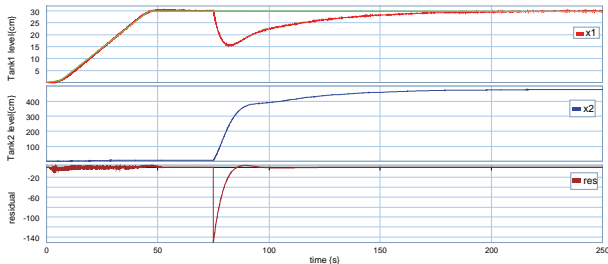


Figure 15. Simultaneous faults,  $\gamma = 1$  and 75% obstruction in the tank2 outlet hole.

## 5. CONTROLLER RECONFIGURATION AND AFTC

This section gives some clues on how to use the method proposed in this paper in the context of AFTC, i.e., when it becomes mandatory, or just convenient, to reconfigure the control law. This is performed on the same case study handled along this paper now considering a structural fault and a sensor fault.

### 5.1.1. Fault in the distribution valve

Consider again the structural fault  $\gamma = 1$  in the distribution valve, i.e., the discharge into tank1 is blocked and all the flow is directed into tank2. This fault has already been simulated with satisfactory results using  $\gamma = \gamma_r = 0.5$  as rated parameter in the controller. However, if the fault were known it could be of interest to use the real parameter  $\gamma = 1$  in the control law. This cannot be done using the former laws (15), (17), as the controller is not defined. This calls for controller reconfiguration. The same method presented before can be used to solve the problem, but in this case the virtual prototyping of the power control source should be made over tank2, the only way to causally access the dynamics of tank1. The procedure of obtaining a closed loop equivalent to the TBG is suggested by the virtual BG of Figure 16.

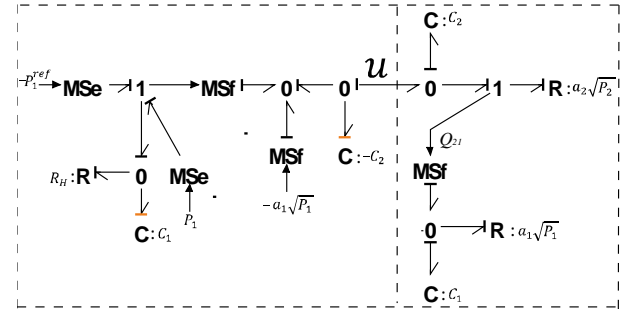


Figure 16. Virtual BG matching the TBG in case of a structural fault in the distribution valve.

The control law obtained reading the BG of figure 16 is:

$$u = -A_2 x_2 + u_2 + u_3 \quad (18)$$

Equation (18) cancels the tank2 dynamics to achieve the TBG. *Mutatis mutandis*, here again an extra integral term can be added to the controller, as shown in the previous section, in order to improve the fault tolerance.

This procedure can be repeated for all structural faults, obtaining a set of control laws which can be switched, with the help of an FDI algorithm, to improve the performance of the control system.

### 5.1.2. Sensor faults and controller reconfiguration

When a fault occurs in the level sensor of tank2, then the control system becomes unobservable. However, the control objectives can still be achieved just discarding the term in (5) that depends on  $x_2$  because  $u_4$

compensates the flows mass differences. But if the level sensor of tank1 fails, then the control must be reconfigured in order to regulate the level of Tank1, because  $x_1$  cannot be injected into the mDBG.

Using the steady state relationship (2) it is possible to define a new TBG to handle faults in sensor level  $x_1$  as depicted in Figure 17.

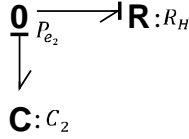


Figure 17. Proposed TBG to handle faults in sensor level  $x_1$ .

$$\dot{x}_{e2} = -\frac{b}{A_2} x_{e2} \quad (19)$$

In the equation above, the tracking error  $x_{e2} = x_2 - x_2^{ref}$  is the state variable of the (incremental) TBG and  $x_2^{ref}$  is the tank1 reference level.  $x_2^{ref}$  is related to  $x_1^{ref}$  through the steady state relationship (2). The same method presented before can be used to solve the problem. Figure 18 shows the associated virtual BG and (20) is the control law obtained.

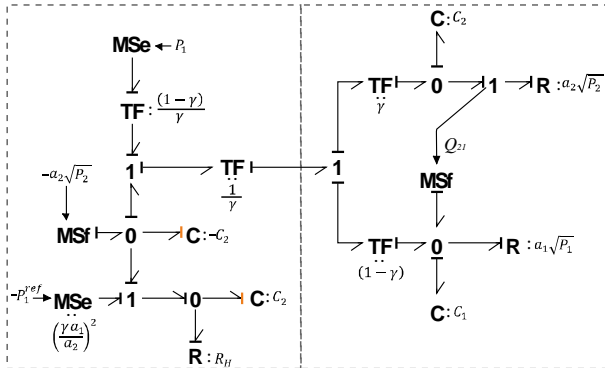


Figure 18. Virtual BG matching the TBG in case of a fault in the sensor level  $x_1$ .

$$u = \frac{1}{\gamma} \left[ -a_2 \sqrt{\rho g x_2} - b \left( x_2 - \left( \frac{a_1}{a_2 \gamma} \right)^2 x_1^{ref} \right) + A_2 \left( \frac{a_1}{a_2 \gamma} \right)^2 \dot{x}_1^{ref} \right] \quad (20)$$

Of course the control systems will follow the reference if and only if only sensor  $x_1$  fails.

Summarizing, controller reconfiguration can be used to get a performance better than that obtained with (15) after a fault occurrence, or in case that the TBG must be modified. As AFTC is beyond the scope of this paper, to get an improved closed-loop behavior with (15) while staying in the context of PFTC, the use of a gain scheduling approach is recommended, performing controller fault accommodation varying the constant  $K$  in dependence on the faults.

## 6. CONCLUSIONS

This work addressed the PFTC approach in the BG domain. The obtained control law is calculated through a energy and power shaping method. An extra term was added to the control law to improve robustness to faults in different components of the control system. Simulations demonstrate the good response and the fault tolerance of the control system.

Further work will be aimed at generalizing the method using the relations between BG and the Port-Controlled Hamiltonian Systems theory.

## ACKNOWLEDGMENTS

The authors wish to thank CONICET (the Argentine National Council for Scientific and Technological Research) and SeCyT-UNR (the Secretary for Science and Technology of the National University of Rosario) for their financial support.

## REFERENCES

- Blanke, M., Kinnaert, M., Lunze, J., Staroswiecki, M. "Diagnosis and Fault-Tolerant Control". Second Edition, Springer-Verlag. 2006.
- Borutzky, W. "Bond graph model-based fault detection using residual sinks". Proceedings of the Institution of Mechanical Engineers, Part I: Journal of Systems and Control Engineering, Volume 223, 2009, pp. 337-352
- Controllab Products B.V., 20-sim, <http://www.20sim.com/>
- Donaire, A. Junco, S. "Energy shaping, interconnection and damping assignment, and integral control in the bond graph domain". Simulation Modelling Practice and Theory 17 (2009) 152-174.
- Isermann, R. "Fault-Diagnosis Systems" Springer-Verlag. 2006.
- Junco, S. "Virtual Prototyping of Bond Graphs Models for Controller Synthesis through Energy and Power Shaping". Conference on Integrated Modeling and Analysis in Applied Control and Automation (IMAACA 2004).
- Johansson, K. "The Quadruple-Tank Process---A multivariable laboratory process with an adjustable zero". IEEE Transactions on Control Systems Technology, 2000.
- Khalil, H. "Nonlinear Systems", Second Edition., Prentice-Hall, New Jersey, 1996.
- Ould Bouamama, B. Samantaray, A. Staroswiecki, M. Dauphin-Tanguy, G. "Derivation of Constraint Relations from Bond Graph Models for Fault Detection and Isolation" Proc. ICBGM 2003.
- Samantaray, A. Medjaher, K. Ould Bouamama, B. Staroswiecki, M. Dauphin-Tanguy, G. "Diagnostic bond graphs for online fault detection and isolation". Simulation Modelling Practice and Theory Volume 14, Issue 3, April 2006, pages 237-262.

- Sontag, E. “*Mathematical Control Theory: Deterministic Finite Dimensional Systems*”. Second Edition, Springer, New York, 1998.
- Sueur, C. Dauphin-Tanguy, G. “*Bond graph approach for structural analysis of MIMO linear systems*”, *Journal of the Franklin Institute*. 328 (1), 1991, pages 55-70.
- Zhang, Y. Jiang. J. “*Bibliographical review on reconfigurable fault-tolerant control systems*” *Annual Reviews in Control*, Vol. 32, No. 2. (December 2008), pages 229-252